Available online at www.sciencedirect.com
ScienceDirect
Journal of the European Ceramic Society 31 (2011) 2089–2098
www.elsevier.com/locate/jeurceramsoc

Preliminary study on suspension plasma sprayed $ZrO_2 + 8$ wt.% Y_2O_3 coatings

Stefan Kozerski [a], Leszek Łatka [a,b], Lech Pawlowski [b,*], Frederico Cernuschi [c], Fabrice Petit [d], Christel Pierlot [e], Harry Podlesak [f], Jean Paul Laval [b]

[a] *Welding Department, Wroclaw University of Technology, ul. Lukasiewicza 5, Pl-50-371 Wroclaw, Poland*
[b] *University of Limoges, SPCTS UMR 6638, European Center of Ceramics, 12, rue Atlantis, 87068 Limoges, France*
[c] *Ricerca sul Sistema Energetico – RSE S.p.A., via Rubattino, 54, I-20134 Milano, Italy*
[d] *Belgium Ceramic Research Centre, 4, av. Gouv. Cornez, B-7000 Mons, Belgium*
[e] *EA 4478 CMF, Ecole Nationale Supérieure de Chimie de Lille, F-59-650 Villeneuve d'Ascq, France*
[f] *Institute of Composite Materials, Chemnitz University of Technology, D-09107 Chemnitz, Germany*

Received 21 January 2011; received in revised form 3 May 2011; accepted 15 May 2011
Available online 8 June 2011

Abstract

$ZrO_2 + 8$ wt.% Y_2O_3 powder of a mean diameter $d_{VS} = 38$ μm was milled to obtain fine particles having mean size of $d_{VS} = 1$ μm. The fine powder was used to formulate a suspension with water, ethanol and their mixtures. The zeta potential of obtained suspensions was measured and found out to be in the range from −22 to −2 mV depending on suspension formulation. The suspension was injected through a nozzle into plasma jet and sprayed onto stainless steel substrates. The plasma spray experimental parameters included two variables: (i) spray distance varying from 40 to 60 mm and (ii) torch linear speed varying from 300 to 500 mm/s. The microstructure of obtained coatings was characterized with scanning electron microscope (SEM) and X-ray diffraction (XRD). The coatings had porosity in the range from 10% to 17% and the main crystal phase was tetragonal zirconium oxide. The scratch test enabled to find the critical load in the range of 9–11 N. Finally, thermal diffusivity of the samples at room temperature, determined by thermographic method, was in the range from 2.95×10^{-7} to 3.79×10^{-7} m^2/s what corresponds to thermal conductivities of 0.69 W/(mK) and 0.97 W/(mK) respectively.

Keywords: Suspension plasma spraying; Yttria stabilized zirconia; Thermal conductivity; Scratch test

1. Introduction

Suspension thermal spraying is a new family of coating deposition methods which uses the finely grained, nanometer and submicrometer sized powder suspension (slurry) as the feedstock.[1,2] At present, the torches generating plasma jets or high velocity combustion flames are used to spray suspensions. The suspension plasma spraying seems to have been most studied by now and it is discussed in present study. As the suspension liquid evaporates during flight in plasma jet; the solids may agglomerate, and, consequently may melt and impact the substrate to build up a coating. The resulting coatings' microstructure depends strongly on the way the suspension is injected to a plasma jet. When suspension is injected through atomizer, the resulting coatings' microstructure is composed of fine grains as shown e.g. by Jaworski et al.[3] When, on the other hand, the suspension is injected mechanically, i.e. enters to the plasma jet as a continuous jet through a nozzle, the microstructure is often composed of two zones: (i) dense zone including well molten lamellas and (ii) sintered one with loosely bound fine grains. *Two zones microstructure* is quite similar to that of coating sprayed using a feedstock prepared by agglomeration by spray-drying of submicrometric and nanometric solids as shown in Fig. 1.

Suspension plasma sprayed yttria stabilized zirconia coatings are being tested in view of their possible application as thermal

* Corresponding author. Tel.: +33 587 50 24 12.
E-mail address: lech.pawlowski@unilim.fr (L. Pawlowski).

0955-2219/$ – see front matter © 2011 Elsevier Ltd. All rights reserved.
doi:10.1016/j.jeurceramsoc.2011.05.014

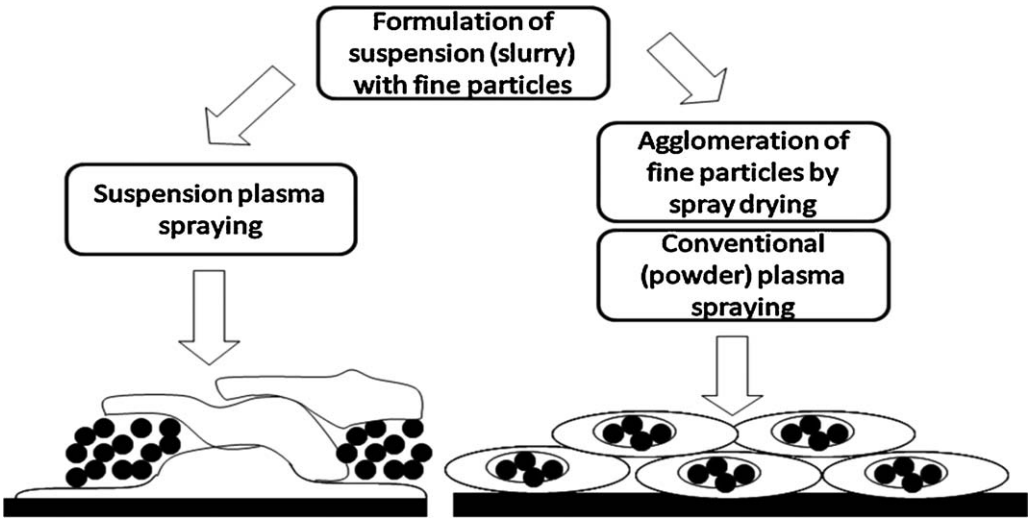

Fig. 1. Two routes leading to a formation of *two zones microstructure*: suspension plasma spraying (a), agglomeration of coarse powders by spray drying followed by conventional (powder) plasma spraying (b).

barrier coatings. This technique may render possible obtaining segmented coatings with high segmentation crack densities and low thermal conductivity. Moreover, the coatings may contain the micro cracks. The possible reason of the cracks' formation was explained by Vaβen et al.[4] The authors discussed the different relaxation processes during spraying. They pointed out that small and thin splats, formed at suspension plasma spraying, would generate low energy release rate generated during cooling of the splat would not give sufficient energy to propagate a crack. Bacciochini et al.[5] analysed suspension sprayed zirconia coatings and investigated such properties as porosity and the pores size as well as their thermal diffusivity. Finally, the mechanical properties of such coatings were characterized using indentation method by Vert et al.[6]

The state of art of thermal transport properties of sprayed coatings was reviewed some time ago.[7] Meanwhile, new testing methods, such as thermographic one used in present paper, have appeared.[8] The present paper presents a preliminary study on characterization of yttria coatings sprayed with the use of suspension injected mechanically to a plasma jet.

2. Experimental methods

2.1. Suspension preparation and injection

Metco 204 NS, a commercially available powder of a composition $ZrO_2 + 8$ wt.% Y_2O_3, prepared by spray drying was used in present study. This powder has been frequently used to obtain thermal barrier coating using conventional spray process (with dry feedstock) and it is a kind of reference in the area. That is why the powder was chosen to be processed in a way described there to form a suspension and used to plasma spraying of coatings which can be compared with the ones prepared in a conventional way.

The volume-surface mean diameter (defined e.g. by Masters [9]) of the coarse powder was measured to be equal to $d_{VS} = 38$ μm. The powder wad ball milled for 14 h until a mean size equal to $d_{VS} = 1$ μm was reached. The distribution of sizes was bimodal size with two maxima at about 0.3 μm and 12 μm (Fig. 2). Longer milling time did not enable to change the size

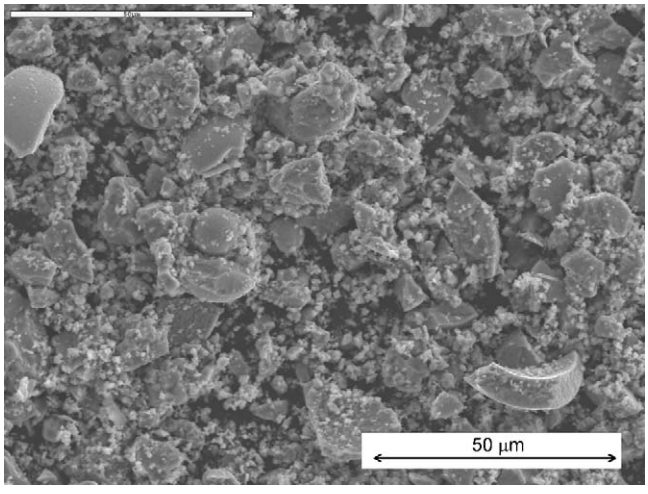

Fig. 2. SEM micrograph (secondary electrons) of ball milled $ZrO_2 + 8$ wt.% Y_2O_3 powder used for suspension formulation.

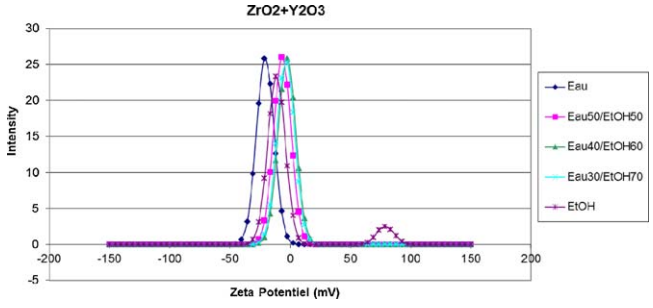

Fig. 3. Zeta potential of the suspension prepared using ball milled $ZrO_2 + 8$ wt.% Y_2O_3 with different liquids.

distribution significantly. The zeta potential of suspensions was measured with a Zetamaster Malvern (Worcestershire, UK), apparatus following standard procedure. The potential is about −22 mV for suspension formulated with water and about −6 mV for a suspension with water mixed with 50 vol.% ethanol (Fig. 3). The final suspension used to spray experiments was formulated with 20 wt.% of powder, 40 wt.% of water and 40 wt. % of ethanol. The suspensions were supplied from a pneumatic system (reservoir) as described elsewhere.[1] Mechanical mixing of suspension was used in order to avoid the agglomeration of fine solids. The static pressure in the container was about 0.040 MPa and the suspension feed rate of about 17 g/min. The suspension was introduced radially inside of a torch's anode – nozzle using a continuous jet injector of ID = 0.5 mm (Fig. 4).

2.2. Plasma spraying

Plasma spraying was performed using a *SG-100* (*Praxair S.T.*, Indianapolis, IN, USA) torch mounted on a 5-axis *IRB-6* robot of *ABB* (Zürich, Switzerland) using an Ar–H_2 (45 − 5 slpm) working gases mixture and electric power of 40 kW. The deposits were sprayed with the torch passes distant 3 mm one to another. After each entire torch scan of a substrate, the deposition was interrupted and the coatings were cooled down to about 40 °C. The suspension sprayed coatings were up to 100 μm thick. Stainless steel substrates (15 mm × 15 mm × 3 mm) were cleaned with ethanol and sand blasted using corundum grit under a pressure of 0.4 MPa before the deposition. The operational process parameters are summarized in Table 1. The spray distance as short as 40 mm was used. Such a short spray distance at suspension plasma spraying results from the small grains sizes which cool down and solidify at shorter spray distances than the used at conventional spraying.[1]

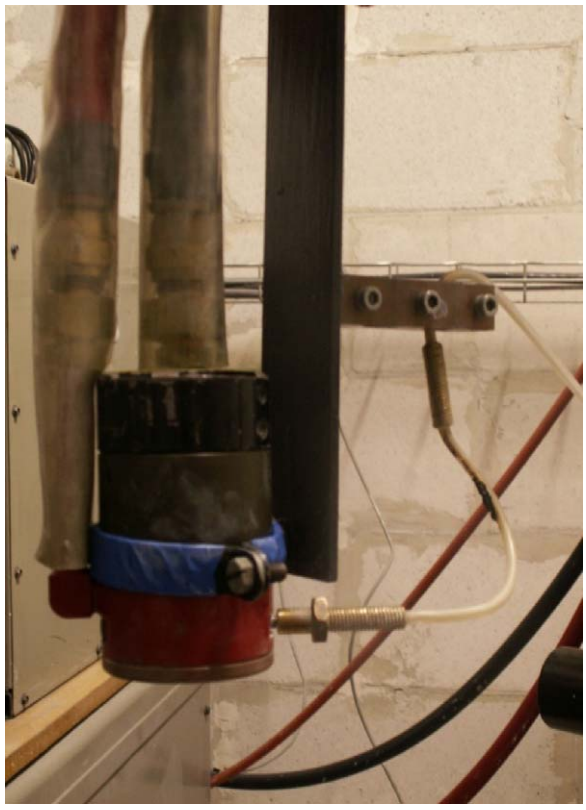

Fig. 4. Set up of internal injection mode with the use of continuous jet nozzle injector installed inside the plasma torch.

2.3. Structure and microstructure characterization

The coatings' cross sections and surfaces were studied using a *ZEISS NEON40* field emission scanning electron microscope (SEM). Cross sections were made by mechanical grinding and polishing. Both cross sections and the surface of coatings were

Table 1
Operational processing parameters used to obtain suspension plasma sprayed ZrO_2 + 8 wt.% Y_2O_3 coatings.

Process parameter	Initial spray parameters	Final spray parameters: experimental runs 1, 2 and 3
Sand blasting		
Sand blasting realized	No	Yes
Plasma spray		
Electric power, kW	40	
Working gases composition	$Ar + H_2$	
Working gases flow rate, slpm	45 + 5	
Spray distance, mm	30–60	60 (run 1); 50 (run 2); and 40 (run 3)
Number of scans	1	27 (run 1); 15 (run 2); and 54 (run 3)
Torch scan speed, mm/s	300–800	300 (run 1); 300 (run 2); and 500 (run 3)
Suspension		
Suspension liquid	Water with ethanol	
Dry powder fraction, mass. % or suspension composition	$20(ZrO_2 + Y_2O_3) + 40C_2H_5OH + 40H_2O$	
Suspension feed rate, g/min	17	
Injection		
Injector type	Nozzle inserted in the torch as shows Fig. 4	
Nozzle injector internal diameter, mm	0.5	
Static pressure in suspension container, MPa	0.04	
Coating		
Thickness, μm		100 (run 1); 70 (run 2); and 110 (run 3)
Temperature of coatings' surface, °C		370–490 (run 1); 420–590 (run 2); and 300–520 (run 3)

Table 2
Operating conditions used in X-ray diffraction tests.

Radiation	CuKα1
Operating conditions	40 kA; 40 mV
Data range (° 2θ)	15–120
Counting step (° 2θ)	0.01
Counting time (s/step)	5

coated with a carbon film to achieve electrical conduction of observed surfaces. The characterization of the samples, used in the determination of thermophysical properties, was made by the field emission scanning electron microscope of *MIRA XMH* (*Tescan*, Brno, CK). The coatings' porosity was evaluated using image analyser type *Screen Measurement* (*Laboratory Imaging Ltd*., Praha, CZ). Eight images, made under a magnification of 1500x using back scattered electrons detector, were made on the samples' cross-sections for each tested sample. The coatings' thickness was said to be a mean value of 30 measurements made on a cross section of the sample. X-ray diffraction patterns were obtained with a *D8 Advance* diffractometer equipped with a fast linear detector *Lynxeye* and using monochromatic Cu Kα1 radiation. The typical recording conditions are reported in Table 2. The *DIFFRAC+* suite of program was used for the preliminary crystal phase analysis and *TOPAS V4.1* for a *Rietveld* method study of sprayed deposits.

2.4. Scratch test

The scratch test was realized with a *MicroCombiTester* (*CSM Instrument,* Peseux, Switzerland) equipped with a Rockwell diamond indenter having a tip radius of 0.2 mm. The scratches were linear with progressively increasing load. The experimental conditions were similar to that presented elsewhere.[10,11] As the coatings were porous, the acoustic signal could not be used for the estimation of critical load, L_c. Instead of that, the load was defined at the onset of the coating loss associated with the beginning of visibility of metallic substrate inside the scratch channel. This measurement was made with help of optical microscope. The tester enabled also to find the friction coefficient at the critical load. The scratch hardness HS_L (GPa) was estimated following the specification of ASTM G171-03 norm:

$$HS_L = \frac{L}{d^2} \tag{1}$$

where L (N) is the applied normal force (30 N was selected) and d (μm) is the corresponding scratch width. The scratch hardness is a fair indicator of coating cohesion.

2.5. Thermal conductivity

The single side thermographic technique, recently developed for non-destructive measurements of thermal diffusivity was used. The details of the method are described elsewhere.[12] Thermal diffusivity α is defined as:

$$\alpha = \frac{\lambda}{\rho c_p} \tag{2}$$

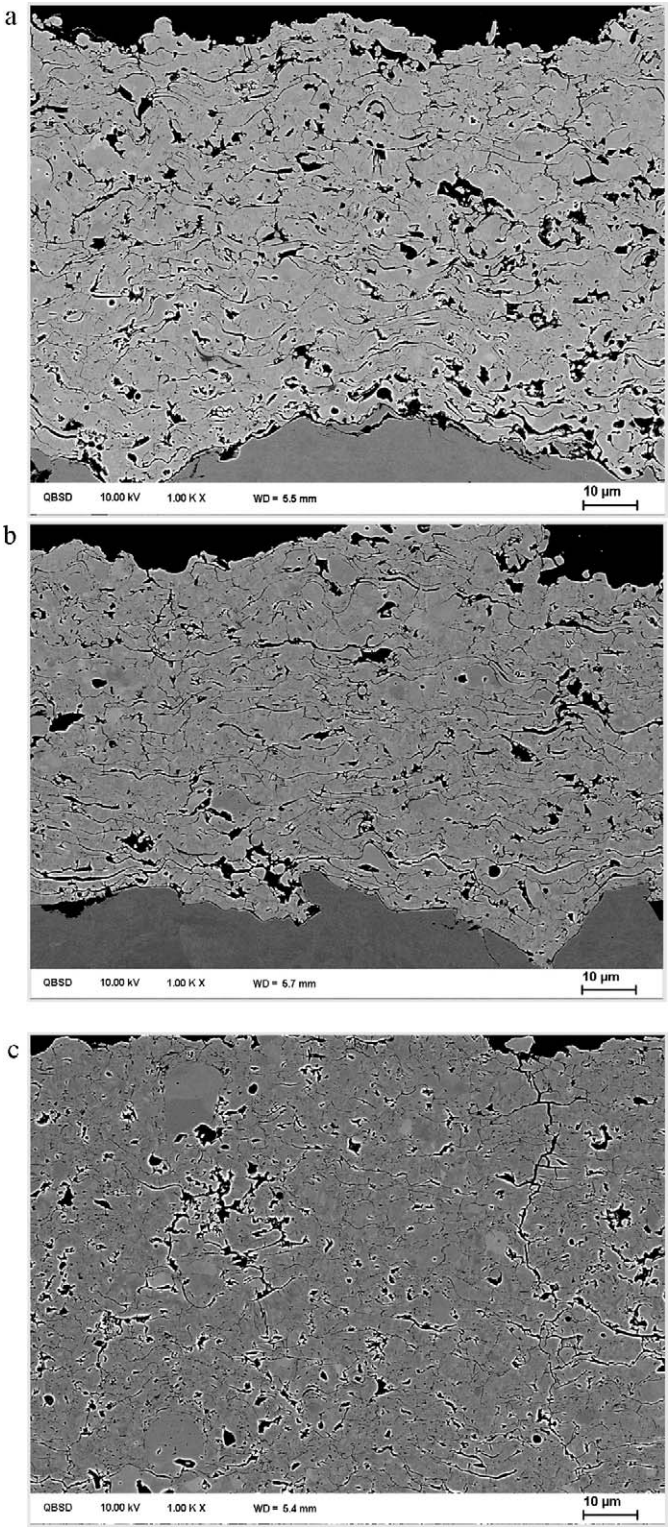

Fig. 5. SEM micrograph (back-scattered electrons) of the cross-sections of the coatings sprayed in run 1 (a), in run 2 (b), and in run 3 (c).

where λ, ρ and c_p are thermal conductivity, the density and the specific heat respectively. Thermal diffusivity of a two-layer sample, coating and metallic substrate, was estimated by fitting the spatial average temperature vs. time, $T(t)$, of the front sample surface after being heated by a laser pulse. Temperature evolution was observed by an infrared camera. The maximum coatings surface temperature increases just few milliseconds after the flash of 10–30 K. The following analytical one-dimensional two layer model was adopted to fit the experimental data:

$$T(t) = \frac{Q_0}{\varepsilon_c \sqrt{\pi t}} \left[1 + 2 \sum_{n=1}^{\infty} \Gamma^n \, e^{-n^2 l_c^2 / \alpha_c t} \right] \tag{3}$$

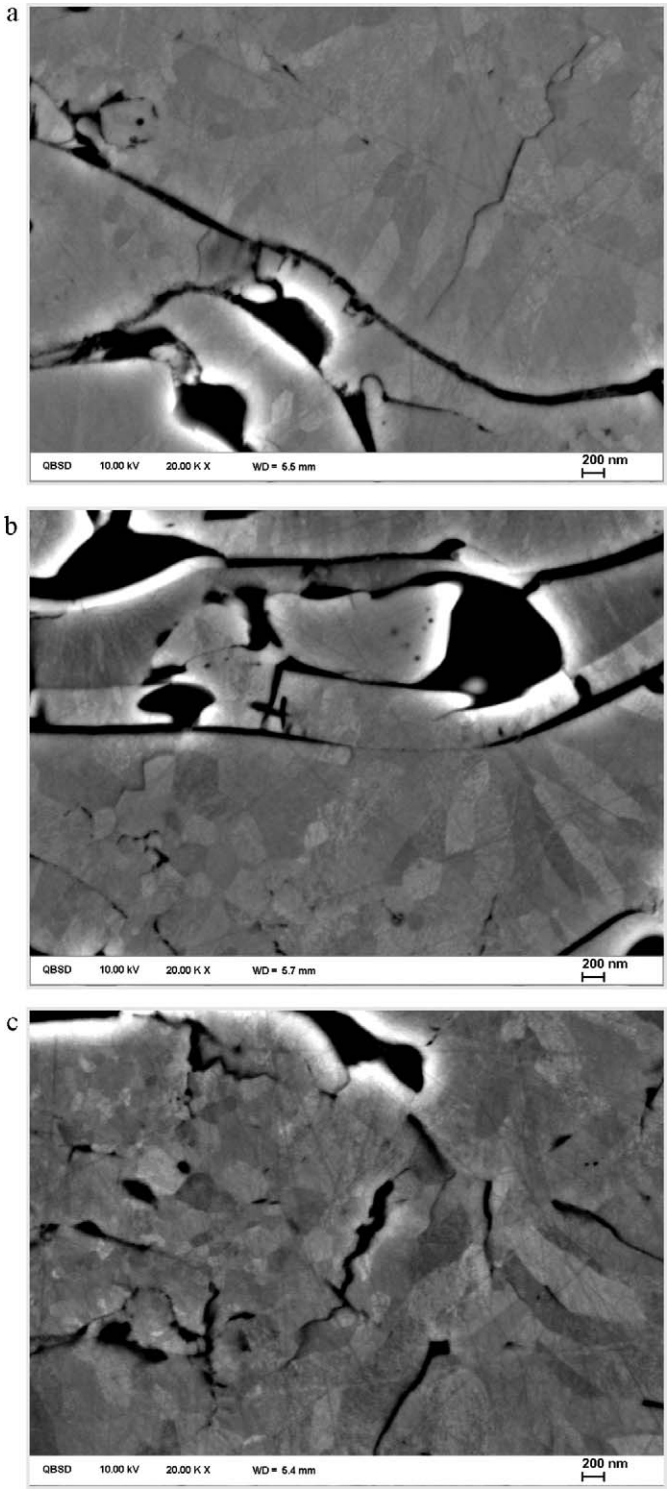

Fig. 6. SEM micrograph (back-scattered electrons) of the cross-section of lamellas inside the coatings sprayed in run 1 (a), in run 2 (b), and in run 3 (c).

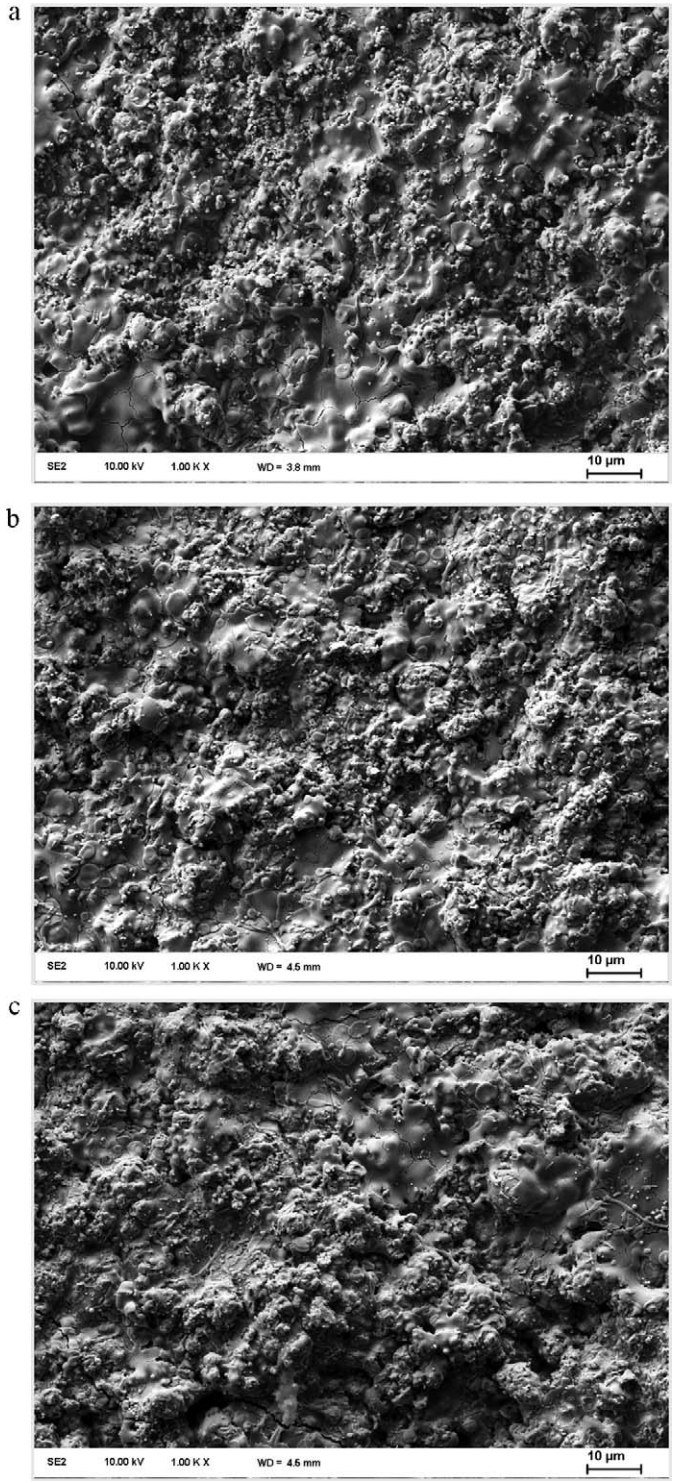

Fig. 7. SEM micrograph (secondary electrons) of the surface of coatings sprayed in run 1 (a), in run 2 (b), and in run 3 (c).

Q_0, $\varepsilon = \sqrt{\lambda \rho C_p}$, $\Gamma = (\varepsilon_c - \varepsilon_s)/(\varepsilon_c + \varepsilon_s)$ and l_c are respectively absorbed energy density, thermal effusivity, reflection coefficient at the interface between coating and substrate and the coating thickness. The lowercases c and s correspond respectively to coating and to substrate. The Nd:YAG laser of (*Theta Industries Inc.*, Port Washington, NY, USA), having wavelength of 1064 nm and pulses duration of 0.8 ms pulses was used in the experiments. The energy of the laser was equal to 2 J. The diameter of the laser beam was equal to 15 mm. An infrared camera type *Jade II LW* by (*CEDIP Infrared Systems*, Croissy-Beaubourg, France) was used to monitor transient temperature of the sample surface after a pulse. The distance corresponding to the duration of heat pulse, defined as:

$$\mu = \sqrt{\alpha t} \tag{4}$$

is close to 1 mm, what is at least 10 times thicker than the thickness of the characterized coatings. Thin layer of colloidal graphite was painted on the coating in order to make it opaque to the laser radiation. The uncertainty of this technique was estimated to 5–7%.[12,13]

3. Results

3.1. Coatings microstructure

The coatings have lamellar structure, similar to that sprayed with coarse feedstock (Fig. 5a–c). The samples obtained in the run 3 have some vertical cracks resulting from relaxation of thermal stresses generated at processing associated with important convective heat input at short spray distance. The lamellar structure could have resulted from the presence of relatively large solid particles in the feedstock (Fig. 2). The cracks were not observed in the coatings sprayed in the runs 1 and 2, i.e. at the spray distances of 60 and 50 mm (runs 1 and 2). On the other hand, the contacts between the lamellas, inside the coating sprayed in the run 3, are better and close porosity clearly smaller. The crystals inside the lamellas have a columnar or an equiaxed shape in the coatings sprayed in the all experimental runs (Fig. 6a–c). The coatings' surface shows *two zones microstructure* with well molten lamellas neighbouring the finely grained zones (Fig. 7a–c). However, the majority of grains were well molten and the sintered zone is not visible in the coatings' cross-sections. The X-ray diffraction diagram shows that the major phase is tetragonal ZrO_2 with a small quantity (about 4 wt.%) of monoclinic phase as shown in Fig. 8. The phase composition of initial powder Metco 204 NS was estimated by Ahmaniemi et al.[14] to be about 82 wt.% tetragonal phase and the rest being monoclinic phase. The presence of cubic zirconia, shown in Fig. 9, can be excluded because of high angular resolution resulting from purely monochromatic X-ray radiation. The proportion of both phases and their lattice parameters determined by the *Rietveld* method are reported in Table 3. The lattice parameters refined for monoclinic zirconia are not very accurate because of low content of this phase (about 4 wt.%). The refined lattice parameters for tetragonal zirconia change only very slightly in three tested samples and are very close to those determined for the deposits obtained using conventional feedstock obtained by Ahmaniemi et al.[14] Theoretical content in Y corresponding to these lattice parameters can be estimated to 8 mol.% Y, giving the formula $Y_{0.08}Zr_{0.92}O_{1.96}$.

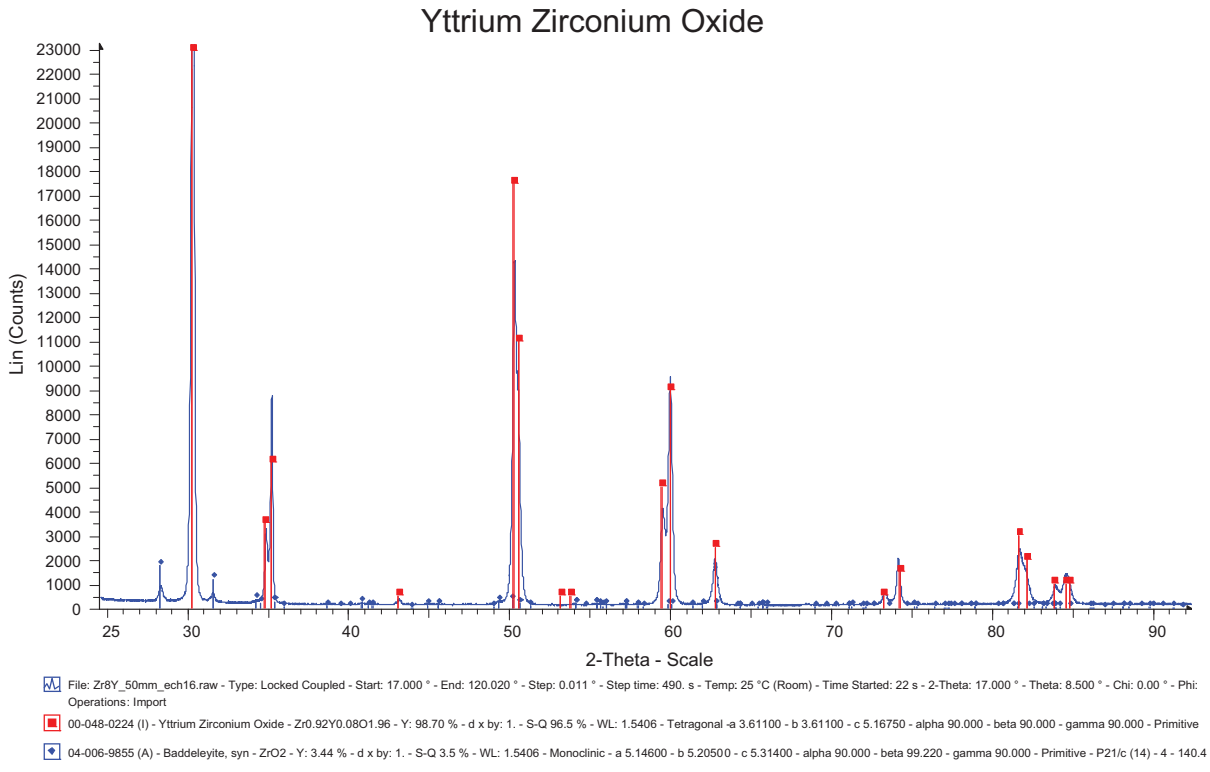

Fig. 8. Typical X-ray diagram of powder of the plasma sprayed coating (sample sprayed in run 2).

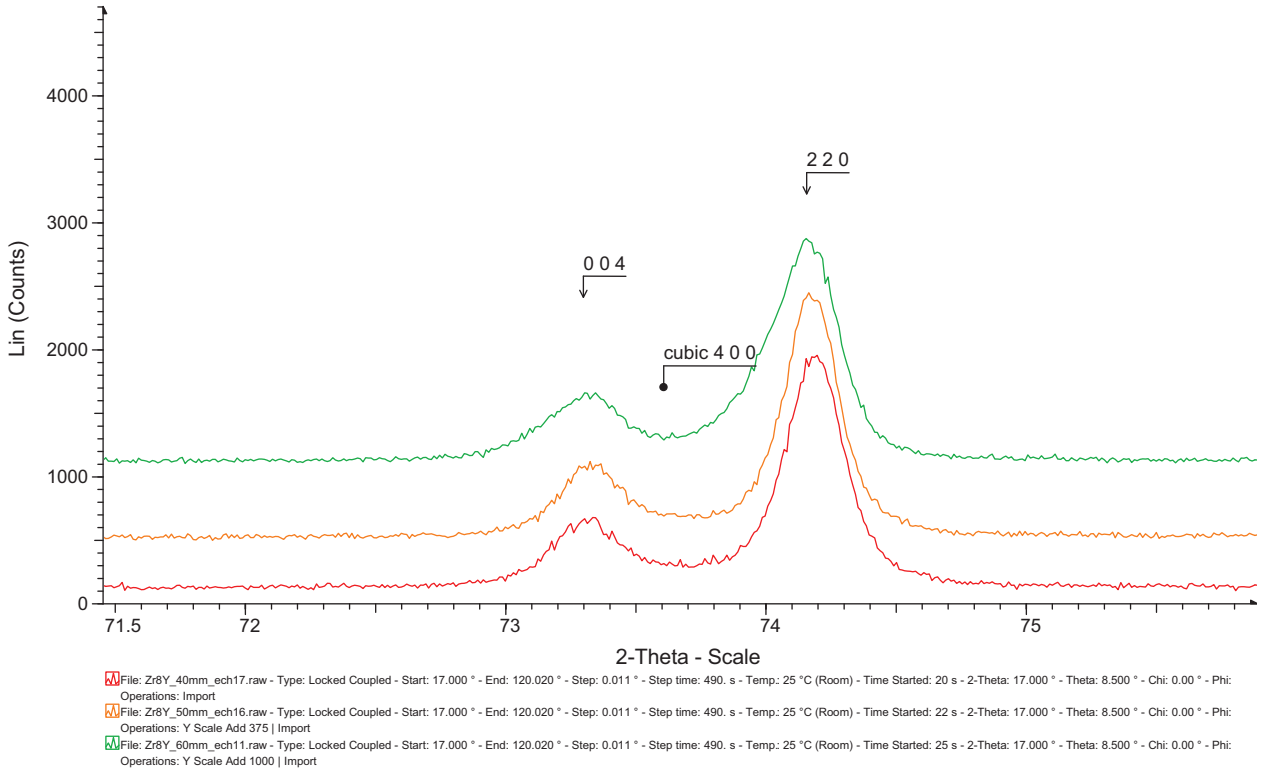

Fig. 9. The part of X-ray diagram of the samples sprayed in the run 1 (top curve), run 2 (middle curve) and in run 3 (bottom curve) showing the absence of the peak corresponding to the cubic phase.

Table 3
Calculation of the content of phases and lattice parameters using *Rietveld* method of zirconia coatings suspension plasma sprayed in different runs.

Sample sprayed in run	Tetragonal zirconia			Monoclinic zirconia		
	Content, wt.%	a, Å	c, Å	Content wt.%	a, b, Å	c, Å and γ,°
1	96.1	3.6158	5.1620	3.9	5.182 5.223	5.282 99.10°
2	96.5	3.6158	5.1625	3.5	5.180 5.199	5.314 99.13°
3	95.6	3.6165	5.1651	4.4	5.180 5.204	5.312 99.08°

3.2. Scratch test

The results of the scratch test are collected in Table 4. Two samples were tested for each experimental run and three scratches were made on each sample. The penetration depth was measured at the load at 24 N. The scratch hardness, HS_L was measured at the load 30 N. The results show that the samples sprayed in the same experimental runs are very different. Some of them are harder than 4 GPa and the critical force is greater than 30 N. The others have the hardness as low as 0.5 GPa and the critical force close to 10 N.

Table 4
Results of the scratch test in which the parameters are mean values of three measurements with the standard deviation of the measurements.

Experimental run	Sample	Penetration depth at force of 24 N, μm	Critical force, N	Scratch hardness, HS_L, GPa
1	1	25.5 ± 4.6	Greater than 30 N	4.8 ± 0.3
	2	49.3 ± 4.7	8.5 ± 0.6	0.51 ± 0.02
2	1	17.4 ± 1.4	–	–
	2	35.3 ± 1.8	–	–
3	1	15.4 ± 1.1	Greater than 30 N	4.1 ± 0.5
	2	54.5 ± 5.2	10.7 ± 1.1	0.63 ± 0.04

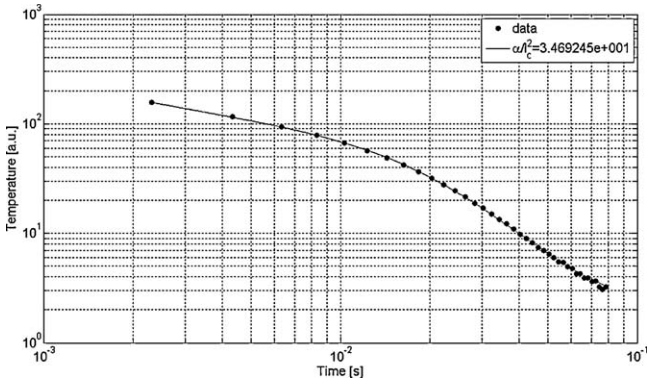

Fig. 10. Evolution of surface temperature as a function of time at the measurements and the best fitting curve for estimating the *through-the-thickness* thermal diffusivity of sample.

3.3. Thermal conductivity

Thermal diffusivity measurements have been repeated ten times for each test. Fig. 10, taken as an example, shows the experimental surface temperature as a function of time and the best fitting curve for estimating thermal diffusivity of sample. Thermal conductivity was estimated from Eq. (2) taking experimental value of thermal diffusivity the data of other properties found in the literature, namely:

- $c_p = 470$ J/(kg K), found by Refs. 14,15;
- $\rho_0 = 6050$ kg/m^3 for tetragonal YPSZ;
- ρ, was estimated from the relationship $\rho = \rho_0(1 - P)$ in which P is the porosity.

The values of thermal diffusivity and conductivity are shown in Table 5. These values are typical for as sprayed porous nanostructured zirconia coatings.[15] Thermal diffusivity and conductivity increase with increasing the distance of spraying. The coatings sprayed at shortest distance of 40 mm conducts heat better than that sprayed using distance of 60 mm. It can be related to low porosity and good contacts between the lamellas in these coatings (see Figs. 5 and 6).

4. Discussion

The stream of suspension injected, into a plasma jet, breaks up and forms individual droplets. Then, eventually, a secondary breakup follows until the droplets reach their final size (Fig. 11). Then, the evaporation of liquid from the suspension occurs, followed by the agglomeration of small solids and their melting. Finally, the molten particles splash up on the substrate. The previous papers realized by our research group on suspension plasma sprayed oxides such as titania and hydroxyapatite, evidenced the *two zone microstructure* shown schematically in Fig. 1. One zone is composed of well molten lamellas and the second – of agglomerated and sintered particulates. The $ZrO_2 + 8$ wt.% Y_2O_3 coatings suspension sprayed in present paper are composed mainly of well molten lamellas (see Fig. 5a–c) and the small solids are well sintered (Fig. 7a–c). The spray distance, which varied between 40 and 60 mm, seems to have influence the following aspects of the coatings' morphology:

Table 5
Experimentally determined thermal diffusivity (mean values from 10 measurements and standard deviations) and porosity and estimated values of thermal conductivity at room temperature for the samples sprayed in different runs.

Experimental run	TBC thickness, μm	TBC thermal diffusivity, 10^{-7} m^2/s	Porosity, %	Thermal conductivity, W/(mK)
1	67 ± 7	2.95 ± 0.02	17.2 ± 0.8	0.69
2	127 ± 9	3.26 ± 0.02	12.9 ± 1.0	0.81
3	104 ± 8	3.79 ± 0.05	9.6 ± 0.5	0.97

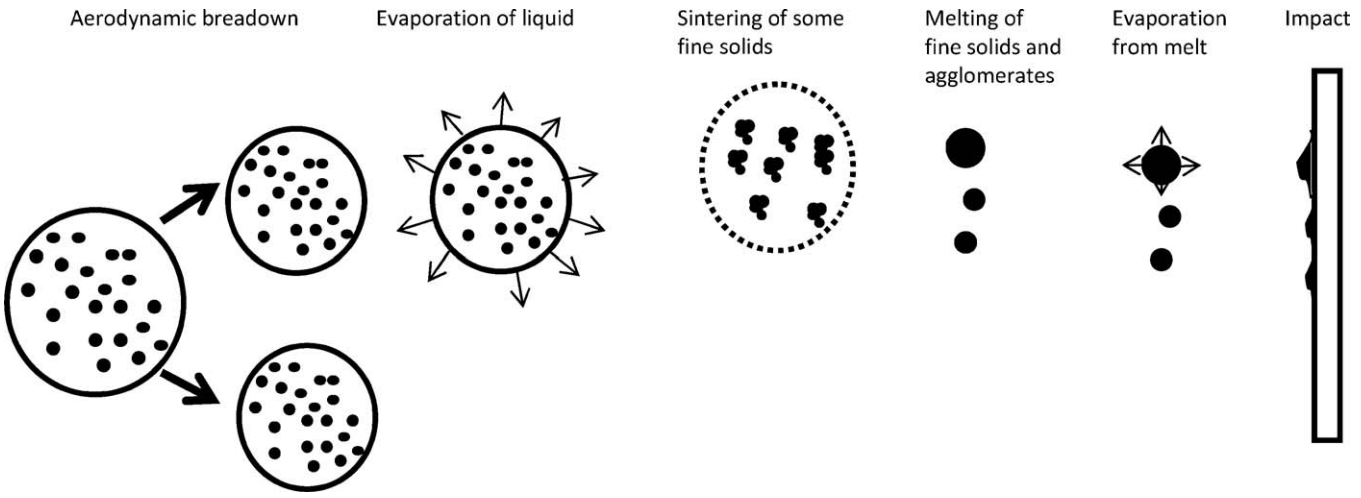

Fig. 11. Evolution of a suspension droplet in the high temperature plasma jet.[1]

- contacts between the lamellas are better when sprayed using short spray distance as shows the comparison between Fig. 6a and c;
- total porosity is smaller in short distance sprayed coatings (see Table 5);
- agglomerated particles which arrive onto the substrate or previously deposited layer at 40 mm spray distance are slightly better molten than that sprayed from the distance of 60 mm (compare Fig. 7a and c);
- vertical cracks going through entire thickness of coatings, resulting from relaxation of thermal stresses, are visible in the coatings sprayed using the distance of 40 mm.

The spray distance of 40 mm seems to be optimal as far as the melting of the particles arriving on the substrate is concerned. However, the heat flux at this spray distance can be as great as 30 MW/m^2 when torch is static with regard to the substrate.[16] The flux decreases considerably if spray distance increases, and, if plasma torch moves with regard to substrate. For example, the thermal fluxes measured for the torch moving with the linear velocity of 250–500 mm/s at the spray distances of 70–85 mm were considerably lower (in the range of 0.1–0.5 MW/m^2 after[17]). The heat flux generates thermal stresses which, in turn, may relax forming the cracks in the coatings.

The mechanical properties found with the scratch test revealed mainly great differences between the samples sprayed in the same experimental runs. The difference increased with increasing charge of the scratching indenter. The weak contact between the lamellas and cracks could have been at the origin of small resistance against the indenter. The hardness of best samples, which is between 4 and 5 GPa, is smaller than that of coatings sprayed using the same powder but without milling and without suspension being about $HV_{0.3} = 7.13$ GPa.[14]

Thermal conductivity of suspension sprayed coatings is, at room temperature, in the range of $\lambda = 0.7$–1 W/(mK) depending on the coatings total porosity, which depends, in turn, on the spray distance (see Table 5). The values are considerably lower that reported for dense $ZrO_2 + 8$ wt.% Y_2O_3, i.e. 2 W/(mK).[15] The difference must result from high total porosity of the coatings which includes bad contacts between the lamellas. The small values of thermal conductivity are acceptable in view of possible application of coatings as thermal barriers.

5. Conclusions

Commercial $ZrO_2 + 8$ wt.% Y_2O_3 powder of a mean diameter $d_{VS} = 38$ μm was mill balled to obtain submicrometer and micrometer size particles having mean size of $d_{VS} = 1$ μm and formulated in a suspension based of a mixture of water with ethanol. The potential zeta of obtained suspension was measured to be about −6 mV. The suspension was injected through a nozzle into a plasma jet and sprayed onto stainless steel substrates. The samples were plasma sprayed using torch stand off varying from 40 to 60 mm and plasma torch linear speed varying from 300 to 500 mm/s. The microstructure of sprayed coatings was observed using scanning electron microscope and X-ray diffraction. The coatings had a porosity ranging from 10% to 17% and the main crystal phase was tetragonal zirconium oxide. The scratch test revealed the critical load in the range of 9–11 N but in some samples the critical load was greater than 30 N. Finally, thermal conductivity diffusivity of the samples at room temperature were found to be between 0.69 W/(mK) and 0.97 W/(mK) depending on the spray distance of the coatings. The small values of thermal conductivity render the coatings acceptable for the application as thermal barrier coatings. However, the future research should include the determination of thermal conductivity at higher temperatures. Moreover, further research of the mechanical properties of the coatings should be carried with the use of other than scratch test method to estimate such parameters as coatings' adhesion to the substrates and their modulus of elasticity.

Acknowledgments

The part of the study was financed by the Ministry of Science and Higher Education of Poland, Grant NN503 134138 and by the Research Fund for the Italian Electrical System under the Contract Agreement between RSE (formerly known as ERSE) and the Ministry of Economic Development – General Directorate for Nuclear Energy, Renewable Energy and Energy Efficiency stipulated on July 29, 2009 in compliance with the Decree of March 19, 2009. The French Embassy in Poland financed the stay of Mr. Łatka in France. The authors are grateful to Prof. Thomas Lampke (Technical University of Chemnitz) for the useful discussion about coatings microstructure, to Mr. Stefano Capelli (RSE, Milan, Italy) for realization of porosity estimations using SEM, and to Mr. Maxence Vanderwelle for the initial studies on phase composition by X-ray.

References

1. Pawlowski L. Suspension and solution thermal spray coatings. *Surf Coat Technol* 2009;**203**(1):2807–29.
2. Fauchais P, Montavon G. Latest developments in suspension and liquid precursor thermal spraying. In: Marple BR, Hyland MM, Lau Y-C, Li C-J, Lima RS, Montavon G, editors. *Thermal spray 2009: proceedings of the international thermal spray conference*. Materials Park, USA: ASM Int.; 2009. p. 136–49, doi:10.1361/cp2009itsc0136.
3. Jaworski R, Pawlowski L, Roudet F, Kozerski S, Le Maguer A. Influence of suspension plasma spraying process parameters on TiO_2 coatings microstructure. *J Thermal Spray Technol* 2008;**71**(1):73–81.
4. Vaßen R, Kaßner H, Mauer G, Stöver D. Suspension plasma spraying: process development and applications. In: Marple BR, Hyland MM, Lau Y-C, Li C-J, Lima RS, Montavon G, editors. *Thermal spray 2009: proceedings of the international thermal spray conference*. Materials Park, USA: ASM Int.; 2009. p. 162–7, doi:10.1361/cp2009itsc0162.
5. Bacciochini A, Ben-Ettouil F, Brousse E, Ilavsky J, Montavon G, Denoirjean A, Valette S, Fauchais P. Quantification of void networks of as-sprayed and annealed nanostructured yttria-stabilized zirconia (YSZ) deposits manufactured by suspension plasma spraying. *Surf Coat Technol* 2010;**202**:683–9.
6. Vert R, Chicot D, Dublanche-Tixier C, Meillot E, Vardelle A, Mariaux G. Adhesion of YSZ suspension plasma-sprayed coating on smooth and thin substrates. *Surf Coat Technol* 2010;**205**:999–1003.
7. Pawlowski L, Fauchais P. A review of thermal transport properties of thermally sprayed coatings. *Int Mater Rev* 1992;**37**(6):271–89.

8. Cernuschi F, Bison P, Marinetti S, Campagnoli E. Thermal diffusivity measurement by thermographic technique for the non-destructive integrity assessment of TBCs coupons. *Surf Coat Technol* 2010;**205**:498–505.
9. Masters K. *Spray drying handbook*. 4th ed. London, England: George Godwin; 1985. p. 67.
10. Kozerski S, Pawlowski L, Jaworski R, Roudet F, Petit F. *Two zones microstructure* of suspension plasma sprayed hydroxyapatite coatings. *Surf Coat Technol* 2010;**204**(8):1236–46.
11. Jaworski R, Pawlowski L, Roudet F, Kozerski S, Petit F. Characterization of mechanical properties of suspension plasma sprayed TiO_2 coatings using scratch test. *Surf Coat Technol* 2008;**202**:2544–53.
12. Bison P, Cernuschi F, Grinzato E, Marinetti S, Robba D. Ageing evaluation of thermal barrier coatings by thermal diffusivity. *Infrared Phys Technol* 2007;**49**:286–91.
13. Bison P, Cernuschi F, Grinzato E. In-depth and in-plane thermal diffusivity measurements of thermal barrier coatings by IR camera: evaluation of ageing. *Int J Thermophys* 2008;**29**:2149–61.
14. Ahmaniemi S, Vuoristo T, Mäntylä F, Cernuschi L, Lorenzoni. Modified thick thermal barrier coatings, thermophysical characterization. *J Eur Ceram Soc* 2004;**24**:2669–79.
15. Raghavan S, Wang H, Dinwiddie RB, Porter WD, Mayo MJ. The effect of grain size, porosity and yttria content on the thermal conductivity of nanocrystalline zirconia. *Scripta Mater* 1998;**39**(8): 1119–25.
16. Etchart-Salas R. Projection par plasma d'arc de particules submicroniques en suspension. Approche expérimentale et analytique des phénomènes impliqués dans la reproductibilité et la qualité des dépôts. PhD thesis, University of Limoges; 2007. Available from: http://www.unilim.fr/theses/2007/sciences/2007limo4058/etchart-salas_e.pdf.
17. Łatka L, Goryachev SB, Kozerski S, Pawlowski L. Sintering of fine particles in suspension plasma sprayed coatings. *Materials* 2010;**3**(7):3845–66.